Temperature-induced changes in wheat phosphoproteome reveal temperature-regulated interconversion of phosphoforms

Lam Dai Vu[1,2,3,4,*], Tingting Zhu[1,2,3,4,*], Inge Verstraeten[1,2,§], Brigitte van de Cotte[1,2], IWGSC[5], Kris Gevaert[3,4,#], Ive De Smet[1,2,#,$]

[1]Ghent University, Department of Plant Biotechnology and Bioinformatics, B-9052 Ghent, Belgium

[2]VIB Center for Plant Systems Biology, B-9052 Ghent, Belgium

[3]Department of Biochemistry, Ghent University, B-9000 Ghent, Belgium

[4]VIB-UGent Center for Medical Biotechnology, B-9000 Ghent, Belgium

[5]Lee's Summit, Missouri, USA

[§]Current address: Institute of Science and Technology Austria, 3400 Klosterneuburg, Austria

[*]Equal contribution

[#]Equal contribution

[$]Corresponding author

ABSTRACT

Wheat (*Triticum* ssp.) is one of the most important human food sources. However, this crop is very sensitive to temperature changes. Specifically, processes during wheat leaf, flower and seed development and photosynthesis, which all contribute to the yield of this crop, are affected by high temperature. While this has to some extent been investigated on physiological, developmental and molecular levels, very little is known about early signalling events associated with an increase in temperature. Phosphorylation-mediated signalling mechanisms, which are quick and dynamic, are associated with plant growth and development, also under abiotic stress conditions. Therefore, we probed the impact of a short-term increase in temperature on the wheat leaf and spikelet phosphoproteome. The resulting data set provides the scientific community with a first large-scale plant phosphoproteome under the control of higher ambient temperature, which will be valuable for future studies. Our analyses also revealed a core set of common proteins between leaf and spikelet, suggesting some level of conserved regulatory mechanisms. Furthermore, we observed temperature-regulated interconversion of phosphoforms, which likely impacts protein activity.

KEYWORDS

Wheat, Temperature, Phosphorylation, Signalling, Leaf, Spikelet, Phosphoproteomics

INTRODUCTION

Wheat (*Triticum* ssp.) is one of the most important staple food crops around the world (Hawkesford *et al.*, 2013). However, the current production of wheat is predicted to be not sufficient to satisfy the future demands of the increasing world's population (Hawkesford *et al.*, 2013; Mochida and Shinozaki, 2013; International Wheat Genome Sequencing Consortium (IWGSC), 2014). In addition, the global temperature is predicted to rise throughout the 21st century (IPCC, 2014); and it has been estimated that for each degree (°C) of temperature increase, global wheat production will reduce by 6% impacting food security (Asseng *et al.*, 2015).

Wheat is sensitive to heat stress during all stages of its growth and development (Barber *et al.*, 2015; Akter and Rafiqul Islam, 2017). During wheat vegetative development, traits affected by high temperature include plant height, specific leaf weight, leaf width, relative water content, chlorophyll content and secondary metabolites (Akter and Rafiqul Islam, 2017). Furthermore, generative wheat growth and development are also very susceptible to increased temperatures (Bennett *et al.*, 1971; Sainiab *et al.*, 1983; Saini *et al.*, 1984; Draeger and Moore, 2017). Specifically, when wheat flowers are exposed to heat stress (10°C above the optimum condition) at the stage between ear initiation and anthesis (when anther development goes through meiosis) this causes abnormal development of the pollen grains in the anther and subsequently results in grain yield reduction (Sainiab *et al.*, 1983; Saini *et al.*, 1984; Fischer, 1985; Wardlaw *et al.*, 1989).

So far, transcriptome and proteome profiles were investigated in wheat under heat stress, revealing differences in gene expression and protein levels, respectively (Liu *et al.*, 2015; Wang *et al.*, 2016; Zhang *et al.*, 2017). Often, changes in gene expression for enzymes were in line with changes in the metabolite profiles upon stress (Rizhsky, 2004). Different

metabolites, including organic acids, amino acids, polyols and lipidic compounds, which are beneficial for the plant during heat stress and known to protect the photosynthesis system, are enhanced in conditions of elevated temperature (Guy *et al.*, 2008; Scalabrin *et al.*, 2015; Qi *et al.*, 2017).

Several protein post-translational modifications (PTMs) are linked with plant stresses; but, these PTMs are hardly investigated in the context of temperature stress (Wu *et al.*, 2016; Hashiguchi and Komatsu, 2016). For example, protein phosphorylation is involved in the regulation of a large number of processes, including abiotic stress signalling (Kline *et al.*, 2010; Bonhomme *et al.*, 2012; Nguyen *et al.*, 2012; Zhang *et al.*, 2014*a*,*b*; Kanshin *et al.*, 2015). However, little is known about the phosphoproteome differences in the important crop wheat in vegetative and reproductive organs and during development under high temperature (Kumar *et al.*, 2017). Nevertheless, understanding PTM-mediated signalling cascades associated with an elevated temperature response is essential to gain insight in temperature tolerance and to facilitate future breeding (Rampitsch and Bykova, 2012).

Here, we monitored phosphorylation events in leaves of wheat seedlings and wheat spikelets exposed for 1h to higher temperature, and further analysed the data for biological processes potentially affected by phosphorylation. The information presented here not only improved our understanding about the role of protein phosphorylation in wheat under high temperature stress, but also provided a large number of phosphorylation sites for potentially critical proteins in this process. Furthermore, we observed temperature-regulated interconversion of phosphoforms, especially of neighbouring phosphosites, which likely impacts protein activity.

MATERIAL AND METHODS

Wheat Plant Materials and Growth Conditions

The seeds used in this study were from two bread wheat (*T. aestivum*, AABBDD, 2n = 6x = 42) cultivars, Fielder and Cadenza. The seeds were put on wet paper enclosed by plastic wrap and vernalized as such at 4°C for 3-4 days, and then transferred to room temperature for germination. Seeds that germinated uniformly were selected and grown in plastic pots containing soil at 21°C (Cadenza) or 24°C (Fielder) under 16 h light/8 h dark (100 μE $m^{-2}s^{-1}$ photosynthetically active radiation, supplied by cool-white fluorescent tungsten tubes, Osram), and 65–75% air humidity.

Temperature Treatment

Temperature treatment was performed 8 h after the start of the light period. For the leaf material, Fielder plants at 7 days post germination growing in separate pots were transferred to two incubators and grown at 34°C (high temperature treatment) or 24°C (control temperature) under constant light (100 μE $m^{-2}s^{-1}$ photosynthetically active radiation) for 60 min. For the spikelet samples, Cadenza plants were cultivated in the greenhouse until the booting stage (stage 45 in Zadoks Decimal Code), then transferred to two incubators at respectively 34°C (high temperature treatment) and 21°C (control temperature) under constant light (100 μE $m^{-2}s^{-1}$ photosynthetically active radiation) for 60 min. The leaves of seedlings from Fielder and the spikelets in the middle section of the ears from Cadenza were collected and frozen in liquid nitrogen.

qRT-PCR

Three biological replicates were used per time point. RNA was extracted and purified with the RNeasy Mini Kit (Qiagen) according to the manufacturer's instruction for plant RNA extraction. DNA digestion was done on columns with RNase-free DNase I (Promega). The iScript cDNA Synthesis Kit (Biorad) was used for cDNA synthesis from 1 µg of RNA. qRT-PCR was performed on a LightCycler 480 (Roche Diagnostics) in 384-well plates with LightCycler 480 SYBR Green I Master (Roche) according to the manufacturer's instructions. Two housekeeping genes, *ACTIN* (GenBank locus AB181991.1) and the *CELL DIVISION CONTROL PROTEIN* (*CDC*, GenBank locus Ta.46201) were used for normalization of the expression level of the *HEAT SHOCK PROTEIN*s. All the primers are listed in **Supplemental Table S1**.

Protein Extraction and Phosphopeptide Enrichment

Total protein extraction was conducted on three biological replicate samples (leaf and spikelet material from independent plants) per wheat cultivar according to our previously described procedure with minor modifications (Vu *et al.*, 2017). Details can be found in the **Supplementary Information**. Phosphopeptides were enriched as previously described (Vu *et al.*, 2017).

LC-MS/MS Analysis

Each sample was analysed via LC-MS/MS on an Ultimate 3000 RSLC nano LC (Thermo Fisher Scientific, Bremen, Germany) in-line connected to a Q Exactive mass spectrometer (Thermo Fisher Scientific). The peptides were first loaded on a trapping column (made in-house, 100 µm internal diameter (I.D.) × 20 mm, 5 µm beads C18 Reprosil-HD, Dr. Maisch, Ammerbuch-Entringen, Germany). After flushing the trapping column, peptides were loaded in solvent A (0.1% formic acid in water) on a reverse-phase column (made in-house, 75 µm

I.D. x 250 mm, 1.9 µm Reprosil-Pur-basic-C18-HD beads, Dr. Maisch, packed in the needle) and eluted by an increase in solvent B (0.1% formic acid in acetonitrile) using a linear gradient from 2% solvent B to 55% solvent B in 120 min, followed by a washing step with 99% solvent B, all at a constant flow rate of 300 nl/min. The mass spectrometer was operated in data-dependent, positive ionization mode, automatically switching between MS and MS/MS acquisition for the 5 most abundant peaks in a given MS spectrum. The source voltage was set at 4.1 kV and the capillary temperature at 275°C. One MS1 scan (m/z 400−2,000, AGC target 3×10^6 ions, maximum ion injection time 80 ms), acquired at a resolution of 70,000 (at 200 m/z), was followed by up to 5 tandem MS scans (resolution 17,500 at 200 m/z) of the most intense ions fulfilling predefined selection criteria (AGC target 5×10^4 ions, maximum ion injection time 80 ms, isolation window 2 Da, fixed first mass 140 m/z, spectrum data type: centroid, under-fill ratio 2%, intensity threshold 1.3xE4, exclusion of unassigned, 1, 5-8, >8 positively charged precursors, peptide match preferred, exclude isotopes on, dynamic exclusion time 12 s). The HCD collision energy was set to 25% Normalized Collision Energy and the polydimethylcyclosiloxane background ion at 445.120025 Da was used for internal calibration (lock mass).

Database Searching

MS/MS spectra were searched against the unpublished IWGSC RefSeq v1.0 database for *Triticum aestivum* (137052 entries) (wheat-urgi.versailles.inra.fr/Seq-Repository/Assemblies) with the MaxQuant software (version 1.5.4.1). For comparison, a second search against the earlier version of IWGSC PopSeq PGSB/MIPS v2.2 database (100344 entries), downloaded from wheatproteome.org, was performed. Detailed MaxQuant settings can be found in **Supplementary Information**. All MS proteomics data have been deposited to the ProteomeXchange Consortium via the PRIDE partner repository (Vizcaíno et al., 2014;

Vizcaíno *et al.*, 2016) with the dataset identifier PXD008703. Next, the 'Phospho(STY).txt' output file generated by the MaxQuant search was loaded into the Perseus (version 1.5.5.3) data analysis software available in the MaxQuant package. Proteins that were quantified in at least two out of three replicates from each temperature were retained. Log2 protein ratios of the protein LFQ intensities were centered by subtracting the median of the entire set of protein ratios per sample. A two-sample test with a *p*-value cut-off $p<0.01$ was carried out to test for differences between the temperatures. Besides, phosphopeptides with 3 valid values in one condition and none in the other were also retained and designated "unique" for that condition.

In Silico Analyses

For Gene Ontology (GO) analysis, the protein sequences of all identified phosphoproteins were loaded in the BLAST2GO software and blasted against the NCBI non-redundant protein sequence database of green plants (*Viridiplantae*) with a cut-off E-Value of 10^{-5}. Afterwards, the results were examined for GO annotation and a Fisher's exact test ($p<0.05$) was performed to extract enriched GO terms in the regulated phosphosite dataset. For Motif-X analyses, the Motif-X algorithm (Chou and Schwartz, 2011) was used to extract significantly enriched amino acid motifs surrounding the identified phosphosites. The sequence window was limited to 13 amino acids and foreground peptides were pre-aligned with the phosphosite in the centre of the sequence window. All identified proteins were used as the background dataset. The occurrence threshold was set at the minimum of 20 peptides and the P-value threshold was set at $< 10^{-6}$. Structural modelling of the WD40 domain of *Ta*SPIRRIG was performed in SWISS-MODEL (Arnold *et al.*, 2006; Biasini *et al.*, 2014). The templates for the modelling studies were identified in the automated mode against the SWISS-MODEL template library (PDB: 5HYN). Structure representations were generated using the PyMOL Molecular Graphics System, Version 1.7.4, Schrödinger, LLC (www.pymol.org).

198

199 **RESULTS AND DISCUSSION**

200

201 ***Experimental Set-up for Early Leaf and Spikelet Phosphoproteome Analyses***

202

203 So far, our knowledge on changes in the wheat proteome upon elevated temperature is largely
204 limited to long-term exposures (day- or week-long treatments) (Majoul *et al.*, 2003; Laino *et*
205 *al.*, 2010; Farooq *et al.*, 2011). We were interested in early signalling associated with a milder
206 increase in ambient temperature, and therefore we wanted to profile changes in the
207 phosphoproteome. To determine a suitable time point for proteome sampling, we first probed
208 the expression levels of two *HEAT SHOCK PROTEINs*, since early thermal sensing is largely
209 reflected in the transcription of *HEAT SHOCK PROTEINs* (Xu *et al.*, 2011). Here, we
210 exposed 7 days old wheat seedlings (Fielder) grown at 24°C for a short-term treatment of
211 34°C and harvested whole shoots at different incubation times (**Figure 1A**). Recent evidence
212 in cereal crop plants has demonstrated a link between high temperature sensitivity at booting
213 stage and seed yield (Hedhly *et al.*, 2009; Draeger and Moore, 2017). Hence, we used booting
214 wheat plants (Cadenza) grown at 21°C and exposed to increased ambient temperature (34°C),
215 after which we harvested spikelets at different incubation times (**Figure 1B**). Since
216 developmental stages differ in optimal growth temperature (Porter and Gawith, 1999), we
217 chose different optimal growth temperatures as the control condition for our experiment. We
218 analysed the transcription of *TaHSP70d* and *TaHSP90.1*, which are markers for temperature
219 response (Xue *et al.*, 2014), in both leaf and spikelet samples. We found that the
220 transcriptional response of *TaHSP70d* and *TaHSP90.1* peaks in both samples at 60 min,
221 indicating a maximum of early high temperature response (**Figure 1C-D**). Therefore, to
222 identify early phosphorylation-controlled signalling components associated with a mild

increased temperature in wheat, we subjected both leaf and spikelet samples from the 60 min time point to our phosphoproteomic workflow (Vu *et al.*, 2016).

New wheat reference sequence improves protein identification

Advances in the wheat reference sequence assembly provide a solid basis for proteome studies in wheat (Brenchley *et al.*, 2012; International Wheat Genome Sequencing Consortium (IWGSC), 2014; Luo *et al.*, 2017). Through Ti-IMAC enrichment and subsequent LC-MS/MS analysis, we identified 3822 phosphopeptides containing 5178 phosphorylated amino acids, representing 2213 phosphoproteins in the leaf samples using the unpublished IWGSC RefSeq v1.0 assembly (**Figure 2 and Supplementary Table S2**). In spikelet samples, our workflow led to the identification of 5581 phosphopeptides containing 7023 phosphosites located on 2696 proteins (**Figure 2 and Supplementary Table S3**). As a comparison, we performed a second search using the earlier published protein sequence database based on the draft genome sequences of bread wheat (International Wheat Genome Sequencing Consortium (IWGSC), 2014). The new protein database, based on the unpublished IWGSC RefSeq v1.0 assembly, resulted in an increase of 30% and 34% of identifications compared to the search using the previous search database that identified 3975 and 5234 phosphosites for leaf and spikelet samples, respectively. This seems to correlate with the increase of 36.5% in the number of entries in the new database compared to the old database, supporting the quality of the new wheat reference sequence assembly. To our knowledge, this is currently the largest set of identified phosphosites in the *Triticum* family. The identified phosphosites in this study were added to our PTMViewer (bioinformatics.psb.ugent.be/webtools/ptm_viewer/) (Vu *et al.*, 2016). In addition, we found

several phosphosites that were differentially regulated between normal (21 or 24°C) and increased ambient temperature (34°C) in wheat leaves and spikelets (**Figure 2).**

A Temperature-regulated Wheat Leaf Phosphoproteome

Phosphosites that exhibited valid values in one condition and none in the other indicate a massive change in phosphorylation levels. For the wheat leaves, we could identify 13 phosphosites that only occurred in the 34°C samples and 32 phosphosites unique for the 24°C condition (**Figure 2 and Supplementary Table S4**). On the rest of the wheat leaf dataset, we performed a Student's t-test ($p<0.01$) on phosphosites with at least 2 valid values in any condition (2810 phosphosites), and this resulted in 33 significantly upregulated phosphosites and 63 significantly downregulated phosphosites at high temperature (**Supplementary Table S5**). Proteins with phosphosites uniquely identified in either conditions and significantly deregulated phosphoproteins from the statistical test were combined and analysed for overrepresented GO terms in biological processes (**Figure 3**) and molecular function (**Supplementary Figure S2**). As expected, upregulated phosphoproteins are highly enriched in the GO terms of stress-induced processes such as response to heat, protein folding (Zhu, 2016), response to hydrogen peroxide (Gupta *et al.*, 2016) and glucose transport (Ruan *et al.*, 2010). On the other hand, downregulated phosphoproteins were mainly enriched in positive regulation of translational elongation/termination, and ribosome biogenesis (Cherkasov *et al.*, 2015).

Expression of *HSPs* is rapidly induced in the leaf by increased temperature (**Figure 1C**), as the resulting proteins play crucial roles when plants are exposed to increased temperature (Sun *et al.*, 2002; Kotak *et al.*, 2007). In our leaf data set, we furthermore identified several differential phosphorylation sites of HSPs at 34°C (**Supplementary Table**

S4-5), namely HSP90 (TraesCS2A01G033700.1, *Ta*HSP90) and HSP60-3A (TraesCSU01G009200.1, *Ta*HSP60-3A) were 10.4-fold and 4.6-fold upregulated at S224 and S577, respectively. However, for both proteins, another phosphosite, namely S93 of *Ta*HSP90 and T420 of *Ta*HSP60-3A, was not differentially phosphorylated after 1 h exposure to 34 °C. This suggested that HSP90 and HSP60-3A protein abundance is likely not the basis for the increase in S224 and S577 phosphopeptide increase, respectively.

Noticeably, our dataset indicated that the phosphoproteome of the photosynthesis machinery in wheat leaves is severely affected by high temperature (**Supplementary Tables S4 and S5**). For example, phosphorylation of T33, T37 and T39 of the subunit P of photosystem I (TraesCS2A01G235000.1) was 3.2-fold downregulated after 1 h exposure to 34°C (**Supplementary Table S5**). In addition, an actin-binding protein (TraesCS1D01G422700.2), whose homologue in *Arabidopsis* (CHUP1) is important for proper chloroplast positioning (Oikawa *et al.*, 2008), was found to be considerably less phosphorylated at S157 upon high temperature (**Supplementary Table S4**). Besides, a kinesin-like protein (TraesCS7D01G176200.1, homologous to *Arabidopsis* KAC1) is highly phosphorylated in its kinesin motor domain (S444) in response to high temperature (**Supplementary Table S4**). Both CHUP1 and KAC1 regulate the accumulation of chloroplast actin filaments in *Arabidopsis*, thus facilitating the anchorage of chloroplasts on the plasma membrane. Last, phosphorylation of kinases involved in chloroplast movement such as the phototropin homologues TraesCS5D01G389200.2 and TraesCS2B01G290500.3 (S525 and S294, respectively) was also elevated by heat (**Supplementary Table S4 and S5**).

The post-translational import of chloroplast proteins is a highly regulated process (Strittmatter *et al.*, 2010). Our dataset shows several components of this process to be affected by high temperature. Increased temperature also highly induced the phosphorylation of a wheat homologue (TraesCS5D01G132600.1) of *Arabidopsis* STY46 kinase at S31

297 (**Supplementary Table S4**). In *Arabidopsis*, STY46 and its homologues STY8 and STY17
298 facilitate import of chloroplast preproteins by phosphorylation of their N-terminal transit
299 peptide (Lamberti *et al.*, 2011). On the other hand, many chloroplast proteins are integrated
300 into the chloroplast outer membrane (COM) without any cleavable signal sequence (Hofmann
301 and Theg, 2005). The ANKYRIN REPEAT-CONTAINING PROTEIN 2 (AKR2) interacts
302 with chloroplast specific lipid markers and facilitates the insertion of COM proteins into the
303 chloroplast outer membrane (Kim *et al.*, 2014). It is speculated that the regulatory mechanism
304 of this process involves conformational changes of AKR2 via PTMs (Kim *et al.*, 2014). Here,
305 we showed that phosphorylation of the AKR2 homologue in wheat
306 (TraesCS4A01G328600.1) at S404 is two-fold upregulated in response to higher temperature
307 (**Supplementary Table S5**). While protein import in chloroplasts has been shown to be
308 altered under stress conditions (Dutta *et al.*, 2009; Ling and Jarvis, 2016), our dataset
309 indicated that this response, especially to high temperature, is highly regulated by
310 phosphorylation.

311 In conclusion, our temperature-mediated leaf phosphoproteome pinpointed
312 photosynthesis as a central target of higher temperature and identified several phosphorylated
313 residues on key components for further functional characterization.

314

315 ***A Temperature-regulated Wheat Spikelet Phosphoproteome***

316

317 For the wheat spikelet, we identified 79 phosphosites that are only present in the 34°C
318 samples and 51 phosphosites that are unique for 21°C samples (**Figure 2 and**
319 **Supplementary Table S6**). A Student's t-test ($p<0.01$) was performed on the rest of the
320 wheat spikelet dataset (phosphosites with at least 2 valid values in temperature condition;
321 3949 phosphosites), and this resulted in 114 significantly upregulated phosphosites and 110

significantly downregulated phosphosites at elevated temperature (**Supplementary Table S7**). Proteins with phosphosites uniquely identified in either condition and significantly deregulated phosphoproteins from the statistical test were combined and GO analysis was performed similarly as for the leaf samples (**Figure 4 and Supplementary Figure S3**). The biological processes enriched in leaf samples were also increased here, such as protein folding, response to heat, response to hydrogen peroxide. Similar to the leaf GO enrichment (**Figure 3**), terms associated with translation were predominantly enriched for downregulated phosphoproteins.

Reproductive development in plants is known to be greatly dependent on the epigenetic control of expression of flowering genes (Gan *et al.*, 2013). This often involves histone modifications such as (de)acetylation, methylation and ubiquitination (Lawrence *et al.*, 2016). Here, we found that the phosphorylation of several histone-modifying enzymes was deregulated in response to heat. For example, the phosphoserine 297 of the histone deacetylase TraesCS1A01G445700.3 was 7.1-fold downregulated and the phosphorylation of S762 S763 in the histone-lysine N-methyltransferase TraesCS2A01G262600.1 was 2.4-fold decreased (**Supplementary Table S7**). In contrast, an ubiquitin protease, TraesCS4D01G266600.3, was 2.2-fold more phosphorylated at S31 and T32. Its *Arabidopsis* homologue, *UBP26*, deubiquitinates the histone H2B to regulate floral transition by control the expression of *FLOWERING LOCUS C* (*FLC*) (Schmitz *et al.*, 2008). Furthermore, it has been demonstrated that phosphorylation is crucial for the activity of histone-modifying enzymes (Pflum *et al.*, 2001; Schmitz *et al.*, 2008; Xu *et al.*, 2015).

Another important step in epigenetic control of gene expression is the ATP-dependent restructuring of nucleosomes (Vignali *et al.*, 2000). Phosphorylation of two homologous SWI2/SNF2 class of chromatin remodelling ATPases, TraesCS7D01G206700.3 (at T2492) and TraesCS7B01G110600.1 (at S1668 and S1671), was massively induced by heat

(**Supplementary Table S6**). The *Arabidopsis* homologue, SPLAYED (SYD), is known to be a co-repressor during floral transition (Wagner and Meyerowitz, 2002). In contrast, phosphorylation of S1728 in the SNF2 ATPase TraesCS6B01G048200.2 is 1.7-fold downregulated (**Supplementary Table S7**). Its homologue in *Arabidopsis*, BRAHMA (BRM) plays a pivotal role in controlling flowering time by regulating the expression of *FLC* and inflorescence architecture, mainly via interaction with the transcription factor KNAT1 (Zhao *et al.*, 2015). Interestingly, a wheat homologue of KNAT1, TraesCS5B01G410600.1, was also less phosphorylated at high temperature (**Supplementary Table S7**).

In conclusion, our data suggested that an increase in ambient temperature can alter phosphorylation status of chromatin remodelling proteins as an important mechanism to control gene expression during the reproductive stage. Further, other proteins involved in pollen, pistil or gametophyte development (**Supplementary Tables S6 and S7**) also exhibit altered phosphorylation in response to increased temperature.

Comparison of Leaf and Spikelet Phosphoproteome

In total, we identified 2491 identical phosphosites in both organs, which account for 48% and 35% of all identified phosphosites in leaf and spikelet samples, respectively (**Figure 5**). Only 7 phosphosites were found commonly upregulated at high temperature in both organs and 8 were commonly downregulated in both organs (**Figure 5 and Supplementary Table S8**). Notwithstanding the considerable overlap between the phosphosites identified in both organs, the limited overlap between similarly regulated phosphosites indicated distinct responses in the leaf and spikelet phosphoproteomes at the early stages of thermal signalling.

Among the common higher temperature-induced phosphosites, phosphorylation of S464 of the pseudouridine synthase TraesCS2B01G177000.1 was increased 1.6-fold and 1.9-

fold in leaf and spikelet samples, respectively. Pseudouridylation of mRNA as well as of non-coding RNAs can be induced in stress conditions and is important for the regulation of gene expression, and involved in splicing, translation and decay of mRNA (Karijolich *et al.*, 2015). On the other hand, three different translation initiation factors are present among the commonly regulated proteins with downregulated phosphosites (**Supplementary Table S8)**. This is in agreement with heat stress-triggered overall pausing of translation elongation, and with heat-induced HSP70 protecting cells from heat shock-induced pausing (Shalgi *et al.*, 2014; Merret *et al.*, 2015). Especially, dephosphorylation of translation initiation factors correlates with the reprogramming of translation following thermal stress in wheat (Gallie *et al.*, 1997).

Leaf and Spikelet Phosphoproteome Motif-X Analyses Reveal Distinct Regulation of Phosphorylation Motifs

So far, little is known about the protein kinases and phosphatases involved in temperature signalling (Ding *et al.*, 2015; Yu *et al.*, 2017; Li *et al.*, 2017; Zhao *et al.*, 2017). Therefore, we used the identified phosphosites to reveal potential phosphorylation motifs and associated kinases that may act in a high-temperature responsive manner. The Motif-X algorithm was applied on the set of regulated phosphosites in leaf and spikelet samples separately, using the sequences of all identified phosphoproteins in either organ as reference (**Figure 6**). In the spikelet, the common SP motif was enriched in both upregulated as well as downregulated phosphosites. This suggested that kinases (and phosphatases) targeting those sites are tightly regulating the protein phosphorylation signatures (meaning the specific combination of phosphorylated and non-phosphorylated residues), which impacts on overall protein behaviour, such as protein activity and localization (Salazar and Höfer, 2009). The acidic SD

motif was significantly overrepresented among the upregulated phosphosites (3.61-fold). In contrast, the downregulated phosphosites showed an enrichment in the basic RxxS motif (4.37-fold) (**Figure 6**). This latter trend was also found in the leaf samples (**Figure 6**). Despite that no motif enrichment was obtained for the upregulated phosphosites in leaf, due to the small size of the data set, we identified six SD motifs among these sites, which account for 13% of the upregulated phosphosites in leaves. This was comparable with 14% of the upregulated phosphosites in the spikelet samples which also shows the SD motif. This possibly indicated a common molecular mechanism of higher temperature response via phosphorylation across different organs and different growth stages. While local intracellular parameters such as the pH can slightly vary in a temperature-dependent manner and thus affect the property of amino acid residues around the phosphosites (Wilkinson, 1999; Schönichen *et al.*, 2013), we do not rule out the possibility that certain phosphosites are targeted by a specific set of higher temperature-activated kinases. The acidic motif SD is known to be targeted by MAP kinases (MPKs), receptor-like kinases (RLKs) and calcium-dependent protein kinases (CDPKs), while RxxS is a motif commonly targeted by MAP kinase kinases (M2Ks) (van Wijk *et al.*, 2014). In support of this, we found 6 RLKs among 10 kinases with a higher phosphorylation level at 34°C in the ear, whereas 3 out of 7 kinases with decreased phosphorylation level are predicted to have MAP3K or MAP4K activity **(Supplementary Table S9)**.

Phosphoproteins with multiple deregulated phosphosites

Since the protein phosphosignature will determine protein behaviour (Salazar and Höfer, 2009), we probed the leaf and spikelet phosphoproteome data for proteins that displayed a combination of up and down-regulated phosphosites. We found 13 phosphoproteins in the

spikelet samples and one in the leaf samples that contained both significantly up and downregulated phosphosites (**Table 1**). It is thus very likely that the status of these phosphosites is not affected by changes in the protein level, but rather by higher temperature-dependent activity of associated kinases and phosphatases. These protein phosphatases and kinases might be activated by higher temperature and target the phosphosites independently to generate different phosphoforms of the target protein (**Figure 7A**). However, the phosphorylation and dephosphorylation events might also occur in an interdependent manner upon higher temperature (**Figure 7B**) (Salazar and Höfer, 2009; Nishi *et al.*, 2015). Crosstalk between different or the same type of PTMs is very common (Beltrao *et al.*, 2013; Nishi *et al.*, 2015), but is still not widely explored in plants.

A complex example is the putative protein kinase TraesCS6B01G377500.3 (**Table 1**), which exhibited two phosphosites S711 and S762 that are, respectively, 2.6- and 2.1-fold upregulated in the spikelet samples treated at 34°C. In contrast, a doubly phosphorylated peptide (DFPI***pS***PS***pS***AR, S227 and S230) was detected 2.5-fold higher in the 21°C samples. Further, a single peptide (***pS***SGIETTPAEAEALSK or S***pS***GIETTPAEAEALSK) could only be detected for all 21°C samples, albeit the phosphosite could not be exactly localized (either S768 or S769).

In addition, we also found proteins with multiple phosphosites that showed the same deregulation across different temperature (**Supplementary Table S10**). A large portion of these sites are detected together on the multi-phosphorylated peptides. These phosphosites may work synergistically to control the protein function at elevated temperature or may generate a phosphorylation code for crosstalk between different protein kinases or phosphatases as discussed above. However, in this case, a change in protein level may result in a general change in abundance of phosphopeptide pool. Hence, studying the co-regulation

of these phosphosites will require additional investigation on the abundance of the proteins, e.g. by analysing intact proteins or rather the different proteoforms.

Altogether, our data indicated that multiple phosphorylation/dephosphorylation events of a single protein induced by stress are common and add another level of complexity to our understanding of stress signalling mechanisms in plants.

Temperature-induced interconversion of neighbouring phosphorylation residues

Interestingly, in the spikelet samples, TraesCS5B01G387800.1 (**Table 1**), which is a homologue of the WD40/BEACH domain protein SPIRRIG in *Arabidopsis thaliana*, exhibited two phosphosites in close proximity with opposite differential regulation upon high temperature. The phosphosite S3236 (***pS***PTTTYGGPGLDVQTLEYR) could only be detected at 34°C, whereas the phosphosite T3238 (SP***pT***TTYGGPGLDVQTLEYR) could only be detected at 21°C (**Supplementary Figure 4**). The phosphosites are located in the WD40-repeat domain (**Figure 8A**), which is crucial for interaction of SPIRRIG with the decapping protein DCP1 to regulate mRNA decay upon salt stress in *Arabidopsis* (Steffens *et al.*, 2015).

Inspecting the protein sequence, we found the two phosphorylation sites localized in a sequence window of 10 amino acids of which four are either Ser or Thr (**Figure 8B**). Neither phosphorylation of the two other Thr residues or a hyper-phosphorylated species of the same peptide could be detected. Hence, a combined effect of phosphorylation of individual sites is likely not relevant. While S3236 was conserved and T3238 not conserved among SPIRRIG homologues, we could also find high frequency of Ser and Thr residues in the same sequence windows in other seed plants (**Figure 8B**). While the high occurrence of phosphorylatable sites might help to preserve the functional phosphorylation pool of a particular sequence during evolution, we suspect that the conformational change of the protein upon stimuli such

as heat could lead to the preference for one phosphosite over the other by the same kinase. This might provide a buffering mechanism to maintain the function of the protein by differential phosphorylation of neighbouring amino acid residues depending on the environmental conditions. However, we also do not rule out allosteric or orthosteric regulation between the two phosphosites that might affect the activity of the protein (Nussinov *et al.*, 2012).

For the splicing factor TraesCS2D01G281200.1 (**Table 1**) the phosphorylated peptide containing only S12 (ASAETLARSP***pS***REPSSDPPR) is uniquely detected at 34°C, while the doubly phosphorylated peptide of S10 and S12 (ASAETLAR***pS***P***pS***REPSSDPPR) was 3.4-fold downregulated at the same temperature in the spikelets. We speculate that the phosphoforms of TraesCS2D01G281200.1 may co-exist in a temperature-dependent stoichiometry.

Such interconversion of neighbouring phosphorylation residues (**Figure 8C**) has until now seldom been observed. One example can be found in the cyanobacteria *Synechococcus elongates,* where the circadian clock is controlled by the oscillating phosphorylation equilibrium between a neighbour serine and threonine in the protein kinase KaiC (Rust *et al.*, 2007). This phosphorylation switch between the two residues is modulated by the stoichiometric interaction of KaiC with KaiA and KaiB, in which the pS-KaiC form antagonize KaiA activity, whereas the pT-KaiC form does not. Similarly, a dual phosphorylation switch has been studied in human (Kilisch *et al.*, 2016). To our knowledge, similar phosphorylation modules have not been reported in plants, especially not in the context of stress responses. It is possible that temperature serves as a signalling switch for such a phosphorylation toggle via regulated interaction with at least a protein kinase and/or phosphatase.

CONCLUSION

In conclusion, we provide the scientific community with the first large scale phosphoproteome in plants under the control of higher ambient temperature across different temperature-sensitive organs. An in-depth analysis showed that the photosynthetic machinery in the leaf is highly responsive to increased temperature, while epigenetic regulation in the spikelets seems to be tightly regulated by higher temperature in a phosphorylation-dependent manner during reproductive development. Furthermore, we observed a core set of common proteins between both leaf and spikelet, suggesting some conserved mechanisms in these organs when responding the higher temperature. Nevertheless, we also observed a large portion of organ-specific regulation. Finally, we exposed a, so far, not reported mechanism of interconversion of neighbouring phosphorylation residues, which likely plays a key role in temperature signalling. Taken together, our data set increases the understanding of temperature signalling in plants.

SUPPLEMENTARY DATA

Table S1 Primers used in this study

Table S2 Phosphosites identified in wheat leaves

Table S3 Phosphosites identified in wheat spikelets

Table S4 Phosphosites uniquely present at either 24 °C or 34 °C in wheat leaves

Table S5 Phosphosites significantly deregulated at 34 °C (Students' t-test $p<0.01$) in wheat leaves

Table S6 Phosphosites uniquely present at either 21 °C or 34 °C in wheat spikelets

520 **Table S7** Phosphosites significantly deregulated at 34 °C (Students' t-test p<0.01) in wheat
521 spikelets

522 **Table S8** Phosphosites that is commonly upregulated or downregulated at 34 °C in both
523 leaves and spikelets

524 **Table S9** Kinases with deregulated phosphosites in this study

525 **Table S10** List of proteins with multiple upregulated or multiple downregulated phosphosites

526

527 **Figure S1** Histograms show normal distribution of Log2 Intensity of quantifiable proteins
528 (proteins present in only one of two temperatures or having at least 2 valid values per
529 temperature) in leaf (A) and spikelet (B)

530 **Figure S2** Overpresented GO terms for molecular functions among leaf proteins with (A)
531 upregulated or (B) downregulated phosphosites. Fold-changes are indicated.

532 **Figure S3** Overpresented GO terms for molecular functions among spikelet proteins with (A)
533 upregulated or (B) downregulated phosphosites. Fold-changes are indicated.

534 **Figure S4** Mass spectrum of phosphopeptides containing S3236 (A) and T3238 (B) in
535 SPIRRIG homologue TraesCS5B01G387800.1.

536

537 **ACKNOWLEDGEMENTS**

538

539 We thank Michiel Van Bel for assistance in depositing the data in the PTMViewer. We thank
540 Natalia Nikonorova for fruitful discussions on MS data analyses. L.D.V. is the recipient of a

VIB International PhD program fellowship. T.Z. is supported by a grant from the Chinese Scholarship Council.

REFERENCES

Akter N, Rafiqul Islam M. 2017. Heat stress effects and management in wheat. A review. Agronomy for Sustainable Development **37**, 37.

Arnold K, Bordoli L, Kopp J, Schwede T. 2006. The SWISS-MODEL workspace: a web-based environment for protein structure homology modelling. Bioinformatics **22**, 195–201.

Asseng S, Ewert F, Martre P, *et al.* 2015. Rising temperatures reduce global wheat production. Nature Climate Change **5**, 143–147.

Barber HM, Carney J, Alghabari F, Gooding MJ. 2015. Decimal growth stages for precision wheat production in changing environments? Annals of Applied Biology **166**, 355–371.

Beltrao P, Bork P, Krogan NJ, Van Noort V. 2013. Evolution and functional cross-talk of protein post-translational modifications. Molecular Systems Biology **9**, 1–13.

Bennett MD, Chapman V, Riley R. 1971. The duration of meiosis in pollen mother cells of wheat, rye and Triticale. Proceedings of the Royal Society London. Sereis B, Biological Sciences **178**, 259–275.

Biasini M, Bienert S, Waterhouse A, *et al.* 2014. SWISS-MODEL: modelling protein tertiary and quaternary structure using evolutionary information. Nucleic Acids Research **42**, W252–W258.

Bonhomme L, Valot B, Tardieu F, Zivy M. 2012. Phosphoproteome Dynamics Upon Changes in Plant Water Status Reveal Early Events Associated With Rapid Growth Adjustment in Maize Leaves. Molecular & Cellular Proteomics **11**, 957–972.

Brenchley R, Spannagl M, Pfeifer M, *et al.* 2012. Analysis of the bread wheat genome using whole-genome shotgun sequencing. Nature **491**, 705–710.

Cherkasov V, Grousl T, Theer P, *et al.* 2015. Systemic control of protein synthesis through sequestration of translation and ribosome biogenesis factors during severe heat stress. FEBS Letters **589**, 3654–3664.

Chou MF, Schwartz D. 2011. Biological Sequence Motif Discovery Using *motif-x*. Current Protocols in Bioinformatics, 1–24.

Ding Y, Li H, Zhang X, Xie Q, Gong Z, Yang S. 2015. OST1 kinase modulates freezing tolerance by enhancing ICE1 stability in Arabidopsis. Developmental cell **32**, 278–89.

Draeger T, Moore G. 2017. Short periods of high temperature during meiosis prevent normal meiotic progression and reduce grain number in hexaploid wheat (Triticum aestivum L.). Theoretical and Applied Genetics **130**, 1785–1800.

Dutta S, Mohanty S, Tripathy BC. 2009. Role of Temperature Stress on Chloroplast Biogenesis and Protein Import in Pea. Plant Physiology **150**, 1050–1061.

Farooq M, Bramley H, Palta JA, Siddique KHM. 2011. Heat Stress in Wheat during Reproductive and Grain-Filling Phases. Critical Reviews in Plant Sciences **30**, 491–507.

Fischer RA. 1985. Number of kernels in wheat crops and the influence of solar radiation and temperature. J. agric. Sci., Camb **105**, 447–461.

Gallie DR, Le H, Tanguay RL, Hoang NX, Browning KS, Caldwell C. 1997. Molecular Genetics : The Phosphorylation State of Translation Initiation Factors Is Regulated Developmentally and following Heat Shock in Wheat. Journal of Biological Chemistry **272**, 2–10.

Gan E-S, Huang J, Ito T. 2013. Functional Roles of Histone Modification, Chromatin Remodeling and MicroRNAs in Arabidopsis Flower Development. International Review of Cell and Molecular Biology **305**, 115–161.

591 **Gupta K, Sengupta A, Chakraborty M, Gupta B**. 2016. Hydrogen Peroxide and
592 Polyamines Act as Double Edged Swords in Plant Abiotic Stress Responses. Frontiers in plant
593 science **7**, 1343.
594 **Guy C, Kaplan F, Kopka J, Selbig J, Hincha DK**. 2008. Metabolomics of temperature
595 stress. Physiologia Plantarum **132**, 220–235.
596 **Hashiguchi A, Komatsu S**. 2016. Impact of Post-Translational Modifications of Crop
597 Proteins under Abiotic Stress. Proteomes **4**.
598 **Hawkesford MJ, Araus JL, Park R, Calderini D, Miralles D, Shen T, Zhang J, Parry**
599 **MAJ**. 2013. Prospects of doubling global wheat yields. Food and Energy Security **2**, 34–48.
600 **Hedhly A, Hormaza JI, Herrero M**. 2009. Global warming and sexual plant reproduction.
601 Trends in Plant Science **14**, 30–36.
602 **Hofmann NR, Theg SM**. 2005. Chloroplast outer membrane protein targeting and insertion.
603 Trends in Plant Science **10**, 450–457.
604 **International Wheat Genome Sequencing Consortium (IWGSC)**. 2014. A chromosome-
605 based draft sequence of the hexaploid bread wheat (Triticum aestivum) genome. Science
606 (New York, N.Y.) **345**, 1251788.
607 **International Wheat Genome Sequencing Consortium (IWGSC).** 2014. A chromosome-
608 based draft sequence of the hexaploid bread wheat (Triticum aestivum) genome Ancient
609 hybridizations among the ancestral genomes of bread wheat Genome interplay in the grain
610 transcriptome of hexaploid bread wheat Structural and functional pa. Science (New York,
611 N.Y.) **345**, 1250092.
612 **Kanshin E, Kubiniok P, Thattikota Y, D'Amours D, Thibault P**. 2015. Phosphoproteome
613 dynamics of Saccharomyces cerevisiae under heat shock and cold stress. Molecular systems
614 biology **11**, 813.
615 **Karijolich J, Yi C, Yu YT**. 2015. Transcriptome-wide dynamics of RNA pseudouridylation.

Nature Reviews Molecular Cell Biology **16**, 581–585.

Kilisch M, Lytovchenko O, Arakel EC, Bertinetti D, Schwappach B. 2016. A dual phosphorylation switch controls 14-3-3-dependent cell surface expression of TASK-1. Journal of Cell Science **129**, 831–842.

Kim DH, Park M-J, Gwon GH, *et al.* 2014. An Ankyrin Repeat Domain of AKR2 Drives Chloroplast Targeting through Coincident Binding of Two Chloroplast Lipids. Developmental Cell **30**, 598–609.

Kline KG, Barrett-Wilt GA, Sussman MR. 2010. In planta changes in protein phosphorylation induced by the plant hormone abscisic acid. Proceedings of the National Academy of Sciences **107**, 15986–15991.

Kotak S, Larkindale J, Lee U, von Koskull-Döring P, Vierling E, Scharf KD. 2007. Complexity of the heat stress response in plants. Current Opinion in Plant Biology **10**, 310–316.

Kumar V, Khare T, Sharma M, Wani S. 2017. Engineering Crops for Future: A Phosphoproteomics Approach. Current Protein & Peptide Science **18**, 1–1.

Laino P, Shelton D, Finnie C, De Leonardis AM, Mastrangelo AM, Svensson B, Lafiandra D, Masci S. 2010. Comparative proteome analysis of metabolic proteins from seeds of durum wheat (cv. Svevo) subjected to heat stress. Proteomics **10**, 2359–68.

Lamberti G, Gügel IL, Meurer J, Soll J, Schwenkert S. 2011. The Cytosolic Kinases STY8, STY17, and STY46 Are Involved in Chloroplast Differentiation in Arabidopsis. Plant Physiology **157**, 70–85.

Lawrence M, Daujat S, Schneider R. 2016. Lateral Thinking: How Histone Modifications Regulate Gene Expression. Trends in Genetics **32**, 42–56.

Li H, Ding Y, Shi Y, Zhang X, Zhang S, Gong Z, Yang S. 2017. MPK3- and MPK6-Mediated ICE1 Phosphorylation Negatively Regulates ICE1 Stability and Freezing Tolerance

in Arabidopsis. Developmental cell **43**, 630–642.e4.

Ling Q, Jarvis P. 2016. Analysis of Protein Import into Chloroplasts Isolated from Stressed Plants. Journal of Visualized Experiments.

Liu Z, Xin M, Qin J, Peng H, Ni Z, Yao Y, Sun Q. 2015. Temporal transcriptome profiling reveals expression partitioning of homeologous genes contributing to heat and drought acclimation in wheat (Triticum aestivum L.). BMC Plant Biology **15**, 1–20.

Luo MC, Gu YQ, Puiu D, *et al.* 2017. Genome sequence of the progenitor of the wheat D genome Aegilops tauschii. Nature **551**, 498–502.

Majoul T, Bancel E, Triboï E, Ben Hamida J, Branlard G. 2003. Proteomic analysis of the effect of heat stress on hexaploid wheat grain: Characterization of heat-responsive proteins from total endosperm. PROTEOMICS **3**, 175–183.

Merret R, Nagarajan VK, Carpentier MC, *et al.* 2015. Heat-induced ribosome pausing triggers mRNA co-translational decay in Arabidopsis thaliana. Nucleic Acids Research **43**, 4121–4132.

Mochida K, Shinozaki K. 2013. Unlocking triticeae genomics to sustainably feed the future. Plant and Cell Physiology **54**, 1931–1950.

Nguyen THN, Brechenmacher L, Aldrich JT, *et al.* 2012. Quantitative Phosphoproteomic Analysis of Soybean Root Hairs Inoculated with *Bradyrhizobium japonicum*. Molecular & Cellular Proteomics **11**, 1140–1155.

Nishi H, Demir E, Panchenko AR. 2015. Crosstalk between Signaling Pathways Provided by Single and Multiple Protein Phosphorylation Sites. Journal of Molecular Biology **427**, 511–520.

Nussinov R, Tsai CJ, Xin F, Radivojac P. 2012. Allosteric post-translational modification codes. Trends in Biochemical Sciences **37**, 447–455.

Oikawa K, Yamasato A, Kong S-G, Kasahara M, Nakai M, Takahashi F, Ogura Y,

Kagawa T, Wada M. 2008. Chloroplast Outer Envelope Protein CHUP1 Is Essential for Chloroplast Anchorage to the Plasma Membrane and Chloroplast Movement. Plant Physiology **148**, 829–842.

Pflum MKH, Tong JK, Lane WS, Schreiber SL. 2001. Histone Deacetylase 1 Phosphorylation Promotes Enzymatic Activity and Complex Formation. Journal of Biological Chemistry **276**, 47733–47741.

Porter JR, Gawith M. 1999. Temperatures and the growth and development of wheat: a review. European Journal of Agronomy **10**, 23–36.

Qi X, Xu W, Zhang J, Guo R, Zhao M, Hu L, Wang H, Dong H, Li Y. 2017. Physiological characteristics and metabolomics of transgenic wheat containing the maize C4phosphoenolpyruvate carboxylase (PEPC) gene under high temperature stress. Protoplasma **254**, 1017–1030.

Rampitsch C, Bykova N V. 2012. The beginnings of crop phosphoproteomics: exploring early warning systems of stress. Frontiers in Plant Science **3**, 1–15.

Rizhsky L. 2004. When Defense Pathways Collide. The Response of Arabidopsis to a Combination of Drought and Heat Stress. Plant Physiology **134**, 1683–1696.

Ruan Y-L, Jin Y, Yang Y-J, Li G-J, Boyer JS. 2010. Sugar Input, Metabolism, and Signaling Mediated by Invertase: Roles in Development, Yield Potential, and Response to Drought and Heat. Molecular Plant **3**, 942–955.

Rust MJ, Markson JS, Lane WS, Fisher DS, O'Shea EK. 2007. Ordered Phosphorylation Governs Oscillation of a Three-Protein Circadian Clock. Science **318**, 809–812.

Sainiab HS, Sedgleyc M, Aspinalla D. 1983. Effect of Heat Stress during Floral Development on Pollen Tube Growth and Ovary Anatomy in Wheat (Triticum aestivum L .). Australian Journal of Physiology **10**, 137–144.

Saini HS, Sedgley M, Aspinall D. 1984. Developmental Anatomy in Wheat of Male Sterility

691 Induced by Heat Stress, Water Deficit or Abscisic Acid. Aust. J. Plant Physiol **11**, 243–253.

692 **Salazar C, Höfer T**. 2009. Multisite protein phosphorylation - from molecular mechanisms to
693 kinetic models. FEBS Journal **276**, 3177–3198.

694 **Scalabrin E, Radaelli M, Rizzato G, Bogani P, Buiatti M, Gambaro A, Capodaglio G**.
695 2015. Metabolomic analysis of wild and transgenic Nicotiana langsdorffii plants exposed to
696 abiotic stresses: Unraveling metabolic responses. Analytical and Bioanalytical Chemistry **407**,
697 6357–6368.

698 **Schmitz RJ, Tamada Y, Doyle MR, Zhang X, Amasino RM**. 2008. Histone H2B
699 Deubiquitination Is Required for Transcriptional Activation of FLOWERING LOCUS C and
700 for Proper Control of Flowering in Arabidopsis. PLANT PHYSIOLOGY **149**, 1196–1204.

701 **Schönichen A, Webb BA, Jacobson MP, Barber DL**. 2013. Considering Protonation as a
702 Posttranslational Modification Regulating Protein Structure and Function. Annual Review of
703 Biophysics **42**, 289–314.

704 **Shalgi R, Hurt JA, Krykbaeva I, Taipale M, Lindquist S, Burge CB**. 2014. Widespread
705 inhibition of posttranscriptional splicing shapes the cellular transcriptome following heat
706 shock. **49**, 439–452.

707 **Steffens A, Bräutigam A, Jakoby M, Hülskamp M**. 2015. The BEACH Domain Protein
708 SPIRRIG Is Essential for Arabidopsis Salt Stress Tolerance and Functions as a Regulator of
709 Transcript Stabilization and Localization (X Chen, Ed.). PLOS Biology **13**, e1002188.

710 **Strittmatter P, Soll J, Bölter B**. 2010. The chloroplast protein import machinery: a review.
711 Methods in molecular biology **619**, 307–21.

712 **Sun W, Van Montagu M, Verbruggen N**. 2002. Small heat shock proteins and stress
713 tolerance in plants. Biochimica et Biophysica Acta (BBA) - Gene Structure and Expression
714 **1577**, 1–9.

715 **Thingholm TE, Jensen ON, Larsen MR**. 2009. Analytical strategies for

716 phosphoproteomics. Proteomics **9**, 1451–1468.

717 **Vignali M, Hassan AH, Neely KE, Workman JL**. 2000. ATP-Dependent Chromatin-
718 Remodeling Complexes. Molecular and Cellular Biology **20**, 1899–1910.

719 **Vizcaíno JA, Csordas A, Del-Toro N, *et al.*** 2016. 2016 update of the PRIDE database and
720 its related tools. Nucleic Acids Research **44**, D447–D456.

721 **Vizcaíno et al.** 2014. ProteomeXchange provides globally co-ordinated proteomics data
722 submission and dissemination. **32**, 223–226.

723 **Vu LD, Stes E, Van Bel M, Nelissen H, Maddelein D, Inzé D, Coppens F, Martens L,**
724 **Gevaert K, De Smet I**. 2016. Up-to-Date Workflow for Plant (Phospho)proteomics Identifies
725 Differential Drought-Responsive Phosphorylation Events in Maize Leaves. Journal of
726 proteome research **15**, 4304–4317.

727 **Vu LD, Verstraeten I, Stes E, Van Bel M, Coppens F, Gevaert K, De Smet I**. 2017.
728 Proteome Profiling of Wheat Shoots from Different Cultivars. Frontiers in Plant Science **8**, 1–
729 11.

730 **Wagner D, Meyerowitz EM**. 2002. SPLAYED, a Novel SWI/SNF ATPase Homolog,
731 Controls Reproductive Development in Arabidopsis. Current Biology **12**, 85–94.

732 **Wang X, Xin C, Cai J, Zhou Q, Dai T, Cao W, Jiang D**. 2016. Heat Priming Induces
733 Trans-generational Tolerance to High Temperature Stress in Wheat. Frontiers in Plant Science
734 **7**, 1–12.

735 **Wardlaw IF, Dawson I a., Munibi P, Fewster R**. 1989. The Tolerance of Wheat to High
736 Temperatures Survey Procedures and General Response Patterns. Australian Journal of
737 Agriculture Research **40**, 1–13.

738 **van Wijk KJ, Friso G, Walther D, Schulze WX**. 2014. Meta-Analysis of Arabidopsis
739 thaliana Phospho-Proteomics Data Reveals Compartmentalization of Phosphorylation Motifs.
740 The Plant cell **26**, 2367–2389.

Wilkinson S. 1999. pH as a stress signal. Plant Growth Regulation **29**, 87–99.

Wu X, Gong F, Cao D, Hu X, Wang W. 2016. Advances in crop proteomics: PTMs of proteins under abiotic stress. Proteomics **16**, 847–65.

Xu D, Shan B, Lee B-H, *et al.* 2015. Phosphorylation and activation of ubiquitin-specific protease-14 by Akt regulates the ubiquitin-proteasome system. eLife **4**.

Xu Y, Zhan C, Huang B. 2011. Heat Shock Proteins in Association with Heat Tolerance in Grasses. International Journal of Proteomics **2011**, 1–11.

Xue G-P, Sadat S, Drenth J, McIntyre CL. 2014. The heat shock factor family from Triticum aestivum in response to heat and other major abiotic stresses and their role in regulation of heat shock protein genes. Journal of Experimental Botany **65**, 539–557.

Yu J, Han J, Kim Y-J, *et al.* 2017. Two rice receptor-like kinases maintain male fertility under changing temperatures. Proceedings of the National Academy of Sciences of the United States of America **114**, 12327–12332.

Zhang M, Lv D, Ge P, Bian Y, Chen G, Zhu G, Li X, Yan Y. 2014*a*. Phosphoproteome analysis reveals new drought response and defense mechanisms of seedling leaves in bread wheat (Triticum aestivum L.). Journal of Proteomics **109**, 290–308.

Zhang M, Ma CY, Lv DW, Zhen SM, Li XH, Yan YM. 2014*b*. Comparative phosphoproteome analysis of the developing grains in bread wheat (Triticum aestivum L.) under well-watered and water-deficit conditions. Journal of Proteome Research **13**, 4281–4297.

Zhang Y, Pan J, Huang X, *et al.* 2017. Differential effects of a post-anthesis heat stress on wheat (Triticum aestivum L.) grain proteome determined by iTRAQ. Scientific Reports **7**, 3468.

Zhao C, Wang P, Si T, *et al.* 2017. MAP Kinase Cascades Regulate the Cold Response by Modulating ICE1 Protein Stability. Developmental cell **43**, 618–629.e5.

766 **Zhao M, Yang S, Chen C-Y, Li C, Shan W, Lu W, Cui Y, Liu X, Wu K**. 2015.
767 Arabidopsis BREVIPEDICELLUS Interacts with the SWI2/SNF2 Chromatin Remodeling
768 ATPase BRAHMA to Regulate KNAT2 and KNAT6 Expression in Control of Inflorescence
769 Architecture (X Chen, Ed.). PLOS Genetics **11**, e1005125.

770 **Zhu JK**. 2016. Abiotic Stress Signaling and Responses in Plants. Cell **167**, 313–324.

771
772
773
774
775
776
777
778
779
780
781
782
783
784
785
786
787
788
789
790

FIGURE LEGENDS

Figure 1. Different wheat cultivars and organs used in this study. **(A)** Fielder seedlings are depicted at 7 days after germination. Scale bar, 2.2 cm. **(B)** Cadenza spikelet (inset) is depicted from plants at the booting stage. Red asterisk indicates representative ear used for sampling. Scale bar, 7.5 cm. **(C-D)** Analysis of *HSP70* and *HSP90* expression in both leaf and ear as a proxy for the heat sensing shows a maximum increase at 60 min after transferring to high temperature.

Figure 2. Summary of the phosphoproteome analysis in wheat leaf and ear. T-test significant hits and phosphosites with valid values reproducibly present in only one condition in each organ are collectively analyzed and called as upregulated or downregulated phosphosites.

Figure 3. GO enrichment for biological process in upregulated (A) and downregulated (B) phosphoproteins in leaf samples. All identified leaf phosphosites were used as the background dataset. Fold change is indicated.

Figure 4. GO enrichment for biological process in upregulated (A) and downregulated (B) phosphoproteins in ear samples. All identified ear phosphosites were used as the background dataset. Fold change is indicated.

Figure 5. Venn diagrams showing the number of common identified phosphosites as well as deregulated phosphosites in leaf and ear samples.

Figure 6. Motif-X analysis show an enrichment of an acidic phosphomotif among upregulated phosphosites and of a basic motif among downregulated phosphosites in leaf and ear. Fold-change of the enrichment compared to the background dataset are indicated. N/A, not available.

Figure 7. Heat-dependent phosphorylation and dephosphorylation on a single target protein. **(A)** Heat activates both the kinase and the phosphatase to target different Ser or Thr residues simultaneously, generating different phosphoforms of the protein. **(B)** First, heat activates the phosphatase or kinase. The dephosphorylation or phosphorylation of the protein serves as a crosstalk signal for a second kinase or phosphatase to operate, generating one single phosphoform of the protein.

Figure 8. (A) Structural model of the WD40 domain of Triticum aestivum SPIRRIG (TraesCS5B01G387800.1). The Ser/Thr rich sequence is highlighted in green showing the two phosphosites detected in the study. **(B)** Alignment of SPIRRIG homologues from different plant species. The Ser/Thr-rich window is marked with the Ser/Thr residues highlighted in yellow. Domain prediction was performed in Interpro (www.ebi.ac.uk/interpro/). **(C)** Model of temperature-induced interconversion of neighboring phosphosites.

Wheat ID	Upregulated	Fold change (upregulation)	Downregulated	Fold-change (downregulation)	Arabidopsis homologues	Arabidopsis homologue description
TraesCS2A01G209100.1	T1371	5.5	S969	2.7	AT3G60240	CUM2, protein synthesis initiation factor 4G
TraesCS2D01G281200.1	S12*	Unique for 34 °C	S12*	3.4	AT5G51300	ATSF1, nuclear localized splicing factor, involved in alternative splicing of some mRNAs.
			S10	3.4		
TraesCS3A01G538200.1	S1297	Unique for 34 °C	S1126	2.4	AT3G09670	Tudor/PWWP/MBT superfamily protein
TraesCS3B01G212100.3	S771	Unique for 34 °C	T606	Unique for 21 °C	AT5G21160	LARP1a, involved in mRNA degradation in response to heat stress.
TraesCS3D01G178100.1	S5	Unique for 34 °C	S203	5.1	AT3G62330	OXS2, zinc finger family protein
	S6	Unique for 34 °C				
TraesCS3D01G205900.4	S648	Unique for 34 °C	S672	1.6	AT3G06670	SMEK1, forms complex with PP4 proteins to target and dephosphorylate HYL1 which in turn promotes miRNA biogenesis.
TraesCS3D01G230600.1	T4	Unique for 34 °C	S210	Unique for 21 °C	AT1G60690	NAD(P)-linked oxidoreductase
TraesCS4D01G034300.1	S152	1.5	S575	3.5	AT2G41900	CCCH-type zinc finger protein
TraesCS5B01G387800.1	S3236	Unique for 34 °C	T3238	Unique for 21 °C	AT1G03060	SPIRRIG, WD/BEACH domain protein
TraesCS6B01G208900.5	S363	2.0	S439	1.5	AT3G63400	Cyclophilin-like peptidyl-prolyl cis-trans isomerase
	T360	2.0				
TraesCS6B01G377500.3	S711	2.6	S768 /S769	Unique for 21 °C		kinase superfamily protein
	S762	2.1	S227	2.5	AT5G57610	
			S230	2.5		
TraesCS6D01G167200.1	S791	13.9	S424	1.5	AT3G63400	Cyclophilin-like peptidyl-prolyl cis-trans isomerase
	S794	13.9				
	S348	2.0				
	T345	2.0				
TraesCS7B01G002900.1	S460	Unique for 34 °C	S249	3.41	AT5G43310	COP1-interacting protein-like protein
TraesCS5A01G291600.1	S572	Unique for 34 °C	S485	1.38	AT2G33490	hydroxyproline-rich glycoprotein family protein
			S486	1.38		

Table 1. List of phosphoproteins exhibit multiple upregulated and downregulated phosphosites. For TraesCS2D01G281200.1, the peptide containing only phosphorylated S12 is upregulated and the doubly phosphorylated peptide (S12 and S10) is down regulated.

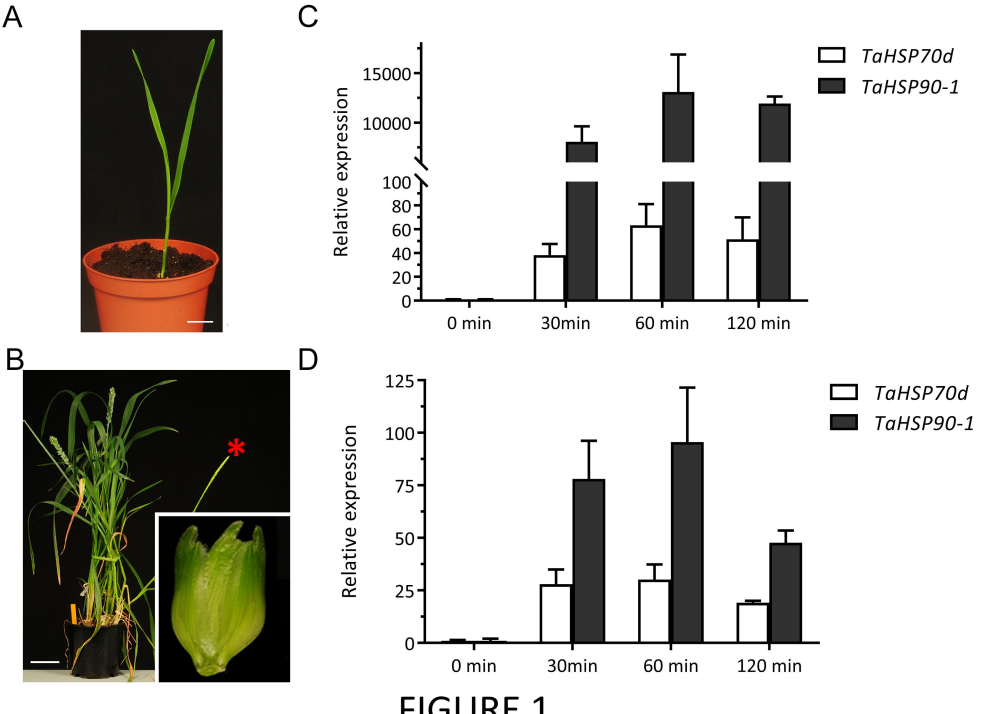
A
B
C
D
Relative expression
15000
10000
100
80
60
40
20
0
0 min
30min
60 min
120 min
TaHSP70d
TaHSP90-1
125
100
75
50
25
0

FIGURE 1

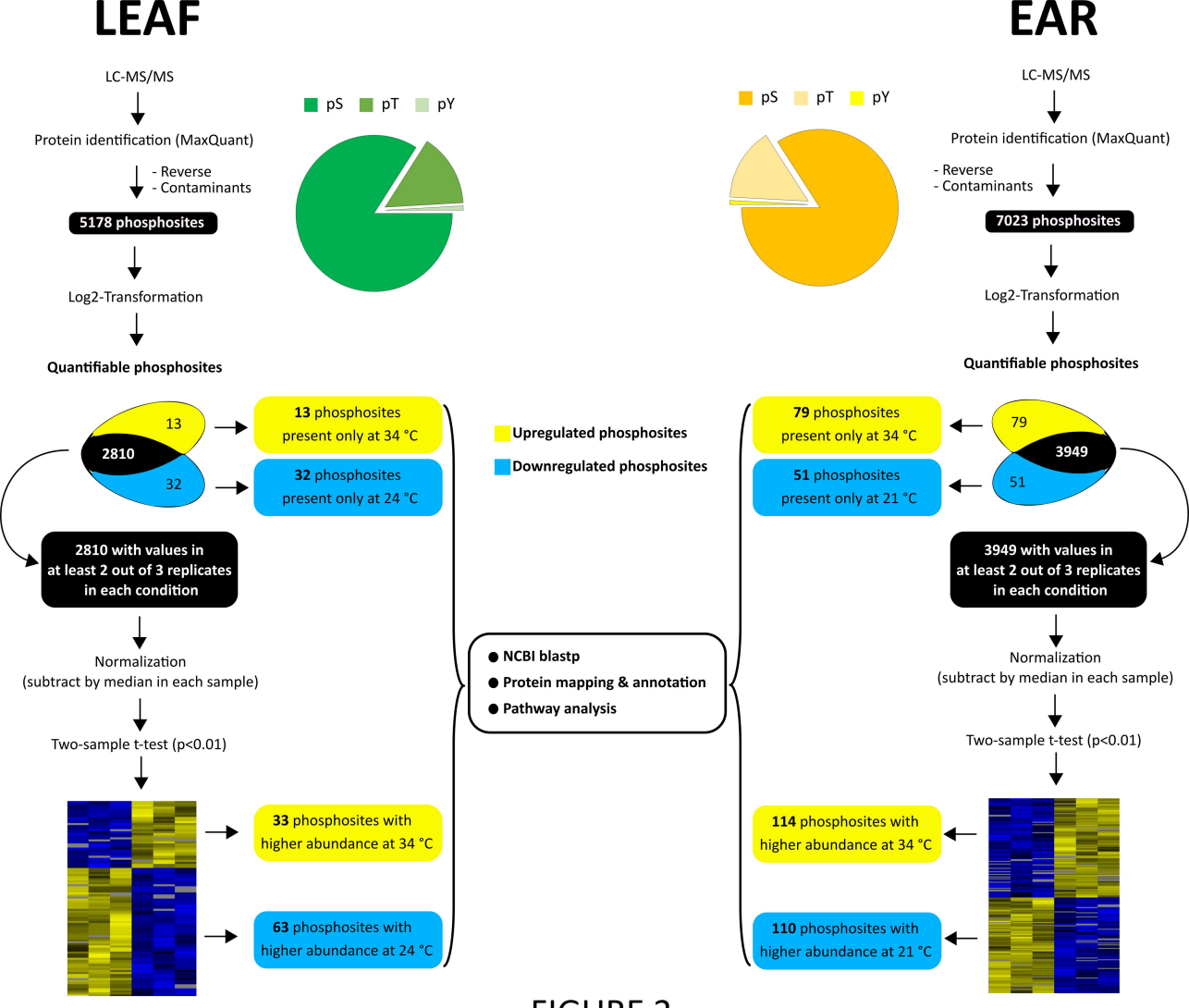
LEAF
LC-MS/MS
Protein identification (MaxQuant)
- Reverse
- Contaminants
5178 phosphosites
Log2-Transformation
Quantifiable phosphosites
pS
pT
pY
13
2810
32
13 phosphosites present only at 34 °C
32 phosphosites present only at 24 °C
2810 with values in at least 2 out of 3 replicates in each condition
Normalization (subtract by median in each sample)
Two-sample t-test (p<0.01)
33 phosphosites with higher abundance at 34 °C
63 phosphosites with higher abundance at 24 °C
Upregulated phosphosites
Downregulated phosphosites
NCBI blastp
Protein mapping & annotation
Pathway analysis
EAR
LC-MS/MS
Protein identification (MaxQuant)
- Reverse
- Contaminants
7023 phosphosites
Log2-Transformation
Quantifiable phosphosites
pS
pT
pY
79
3949
51
79 phosphosites present only at 34 °C
51 phosphosites present only at 21 °C
3949 with values in at least 2 out of 3 replicates in each condition
Normalization (subtract by median in each sample)
Two-sample t-test (p<0.01)
114 phosphosites with higher abundance at 34 °C
110 phosphosites with higher abundance at 21 °C

FIGURE 2

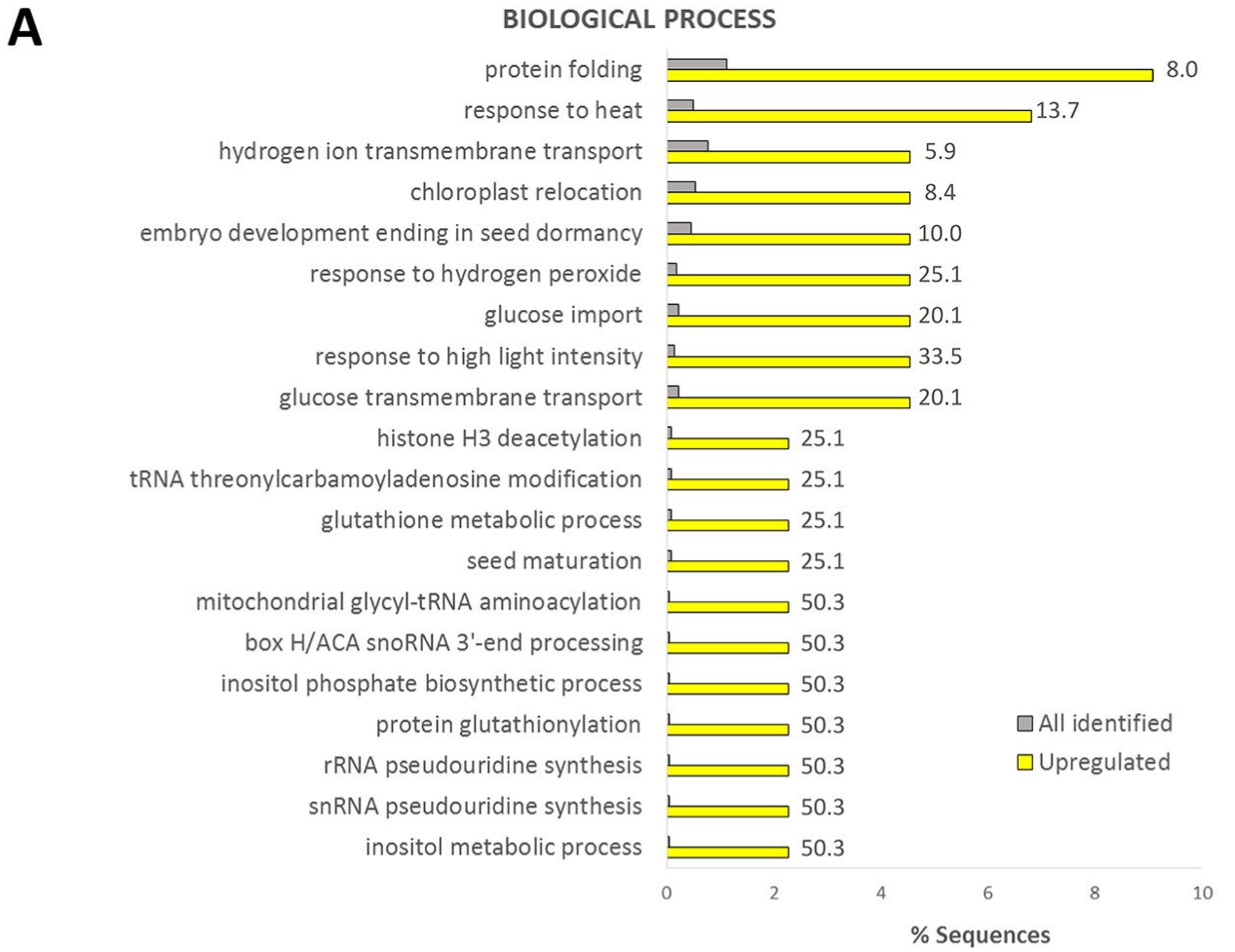
A
BIOLOGICAL PROCESS
protein folding
response to heat
hydrogen ion transmembrane transport
chloroplast relocation
embryo development ending in seed dormancy
response to hydrogen peroxide
glucose import
response to high light intensity
glucose transmembrane transport
histone H3 deacetylation
tRNA threonylcarbamoyladenosine modification
glutathione metabolic process
seed maturation
mitochondrial glycyl-tRNA aminoacylation
box H/ACA snoRNA 3'-end processing
inositol phosphate biosynthetic process
protein glutathionylation
rRNA pseudouridine synthesis
snRNA pseudouridine synthesis
inositol metabolic process
8.0
13.7
5.9
8.4
10.0
25.1
20.1
33.5
20.1
25.1
25.1
25.1
25.1
50.3
50.3
50.3
50.3
50.3
50.3
All identified
Upregulated
0
2
4
6
8
10
% Sequences

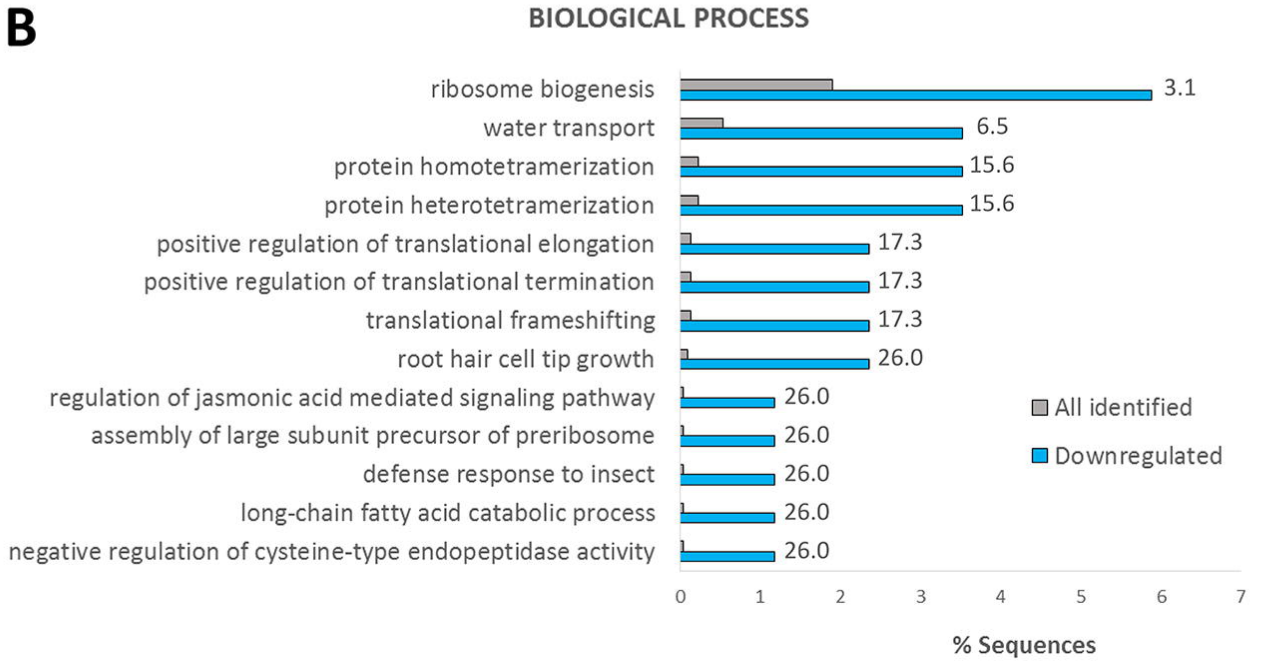
B
BIOLOGICAL PROCESS
ribosome biogenesis
water transport
protein homotetramerization
protein heterotetramerization
positive regulation of translational elongation
positive regulation of translational termination
translational frameshifting
root hair cell tip growth
regulation of jasmonic acid mediated signaling pathway
assembly of large subunit precursor of preribosome
defense response to insect
long-chain fatty acid catabolic process
negative regulation of cysteine-type endopeptidase activity
3.1
6.5
15.6
15.6
17.3
17.3
17.3
26.0
26.0
26.0
26.0
26.0
All identified
Downregulated
0
1
2
3
4
5
6
7
% Sequences

FIGURE 3

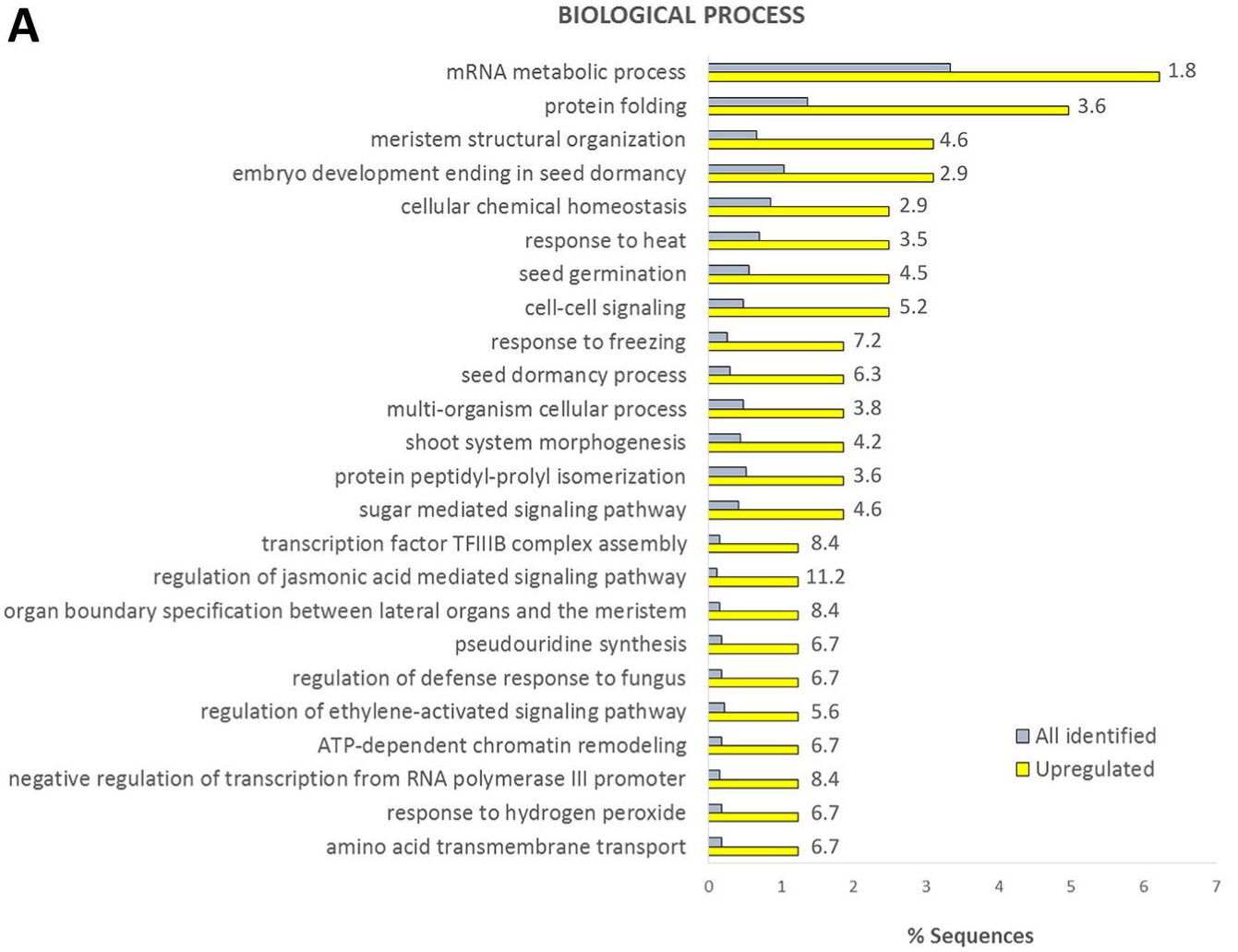
A
BIOLOGICAL PROCESS
mRNA metabolic process
protein folding
meristem structural organization
embryo development ending in seed dormancy
cellular chemical homeostasis
response to heat
seed germination
cell-cell signaling
response to freezing
seed dormancy process
multi-organism cellular process
shoot system morphogenesis
protein peptidyl-prolyl isomerization
sugar mediated signaling pathway
transcription factor TFIIIB complex assembly
regulation of jasmonic acid mediated signaling pathway
organ boundary specification between lateral organs and the meristem
pseudouridine synthesis
regulation of defense response to fungus
regulation of ethylene-activated signaling pathway
ATP-dependent chromatin remodeling
negative regulation of transcription from RNA polymerase III promoter
response to hydrogen peroxide
amino acid transmembrane transport
1.8
3.6
4.6
2.9
2.9
3.5
4.5
5.2
7.2
6.3
3.8
4.2
3.6
4.6
8.4
11.2
8.4
6.7
6.7
5.6
6.7
8.4
6.7
6.7
All identified
Upregulated
0
1
2
3
4
5
6
7
% Sequences

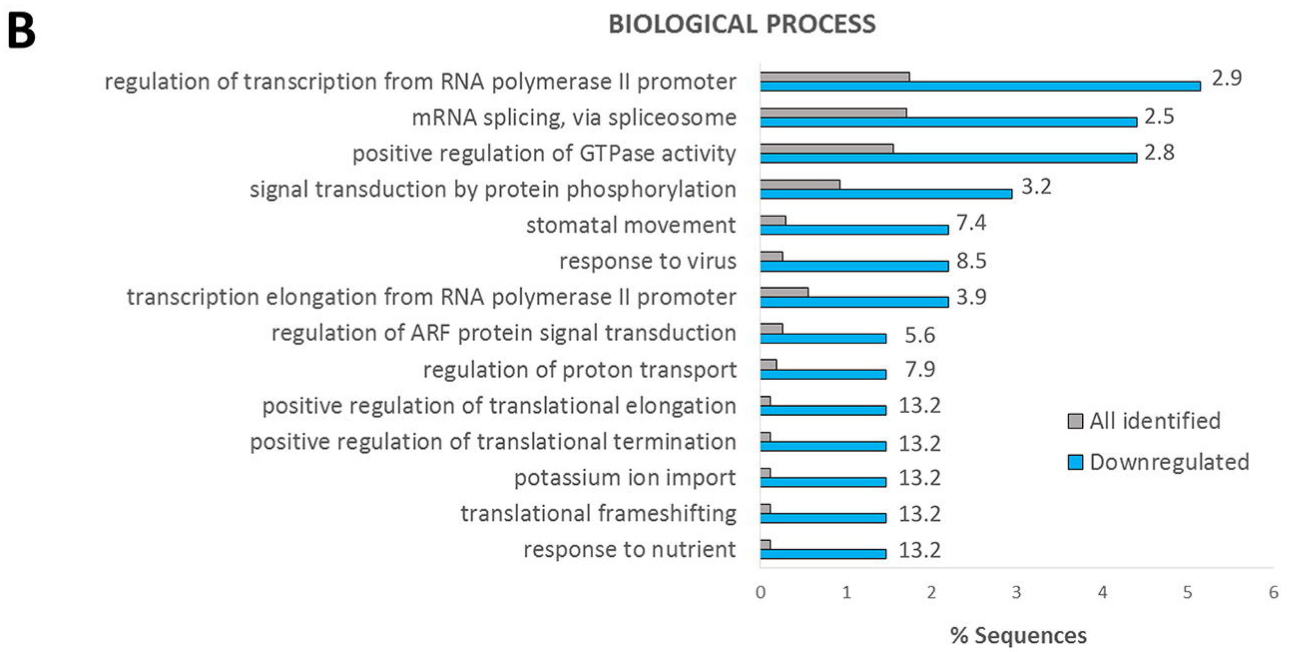
B
BIOLOGICAL PROCESS
regulation of transcription from RNA polymerase II promoter
mRNA splicing, via spliceosome
positive regulation of GTPase activity
signal transduction by protein phosphorylation
stomatal movement
response to virus
transcription elongation from RNA polymerase II promoter
regulation of ARF protein signal transduction
regulation of proton transport
positive regulation of translational elongation
positive regulation of translational termination
potassium ion import
translational frameshifting
response to nutrient
2.9
2.5
2.8
3.2
7.4
8.5
3.9
5.6
7.9
13.2
13.2
13.2
13.2
13.2
All identified
Downregulated
0
1
2
3
4
5
6
% Sequences

FIGURE 4

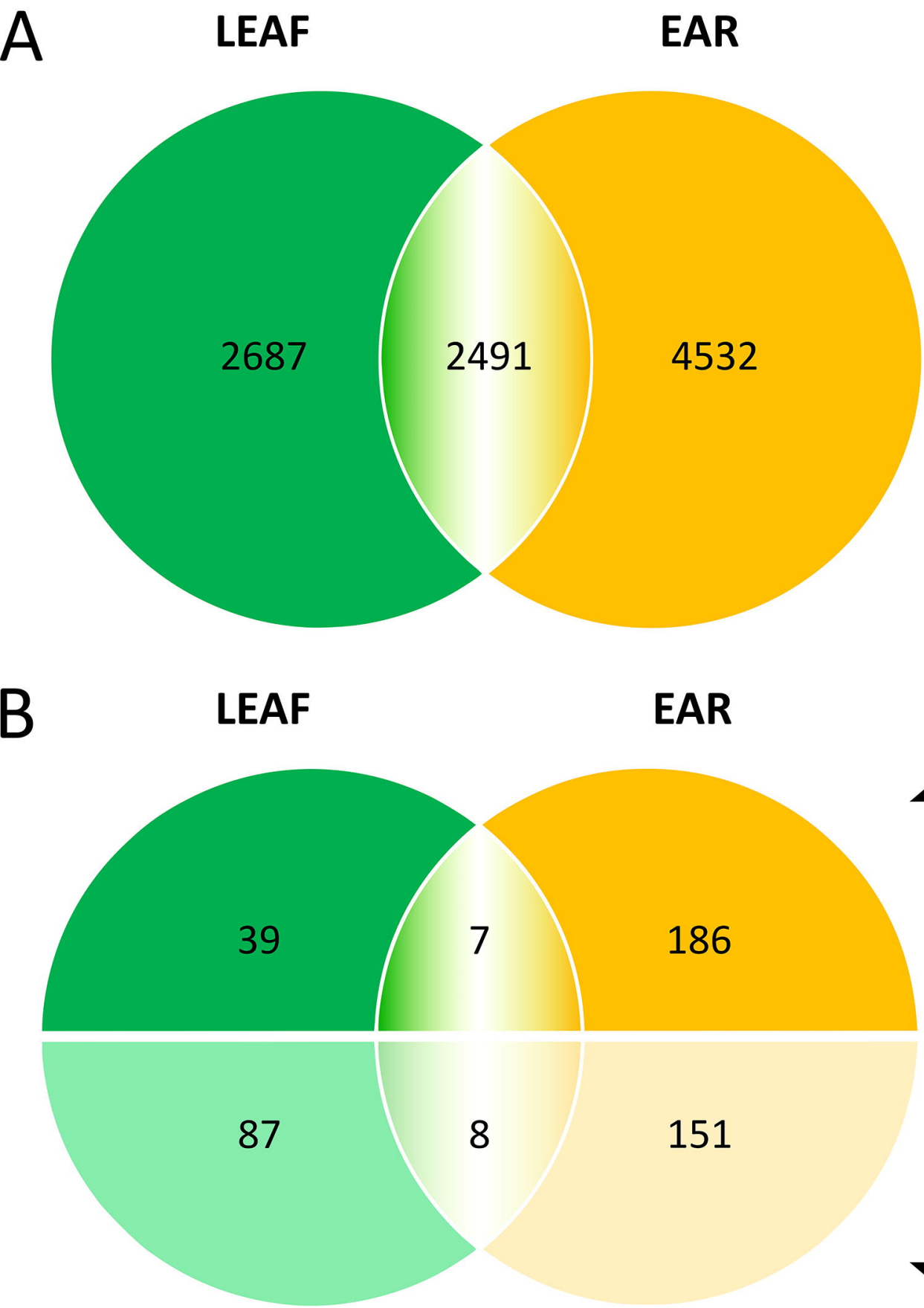
A
LEAF
EAR
2687
2491
4532
B
LEAF
EAR
39
7
186
87
8
151
UPREGULATED
DOWNREGULATED

FIGURE 5

	UPREGULATED		DOWNREGULATED	
EAR	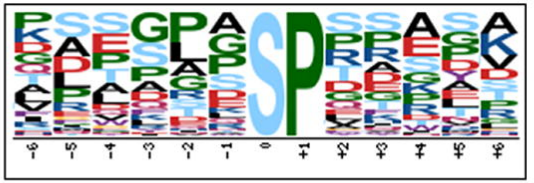	4.48	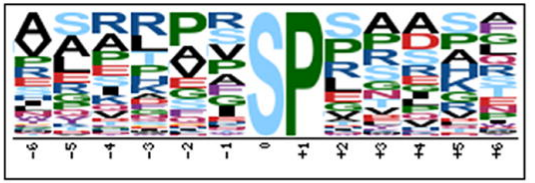	5.14
		3.61		4.37
LEAF	N/A		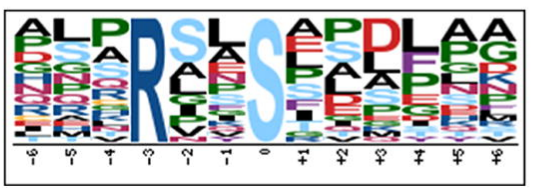	4.82

FIGURE 6

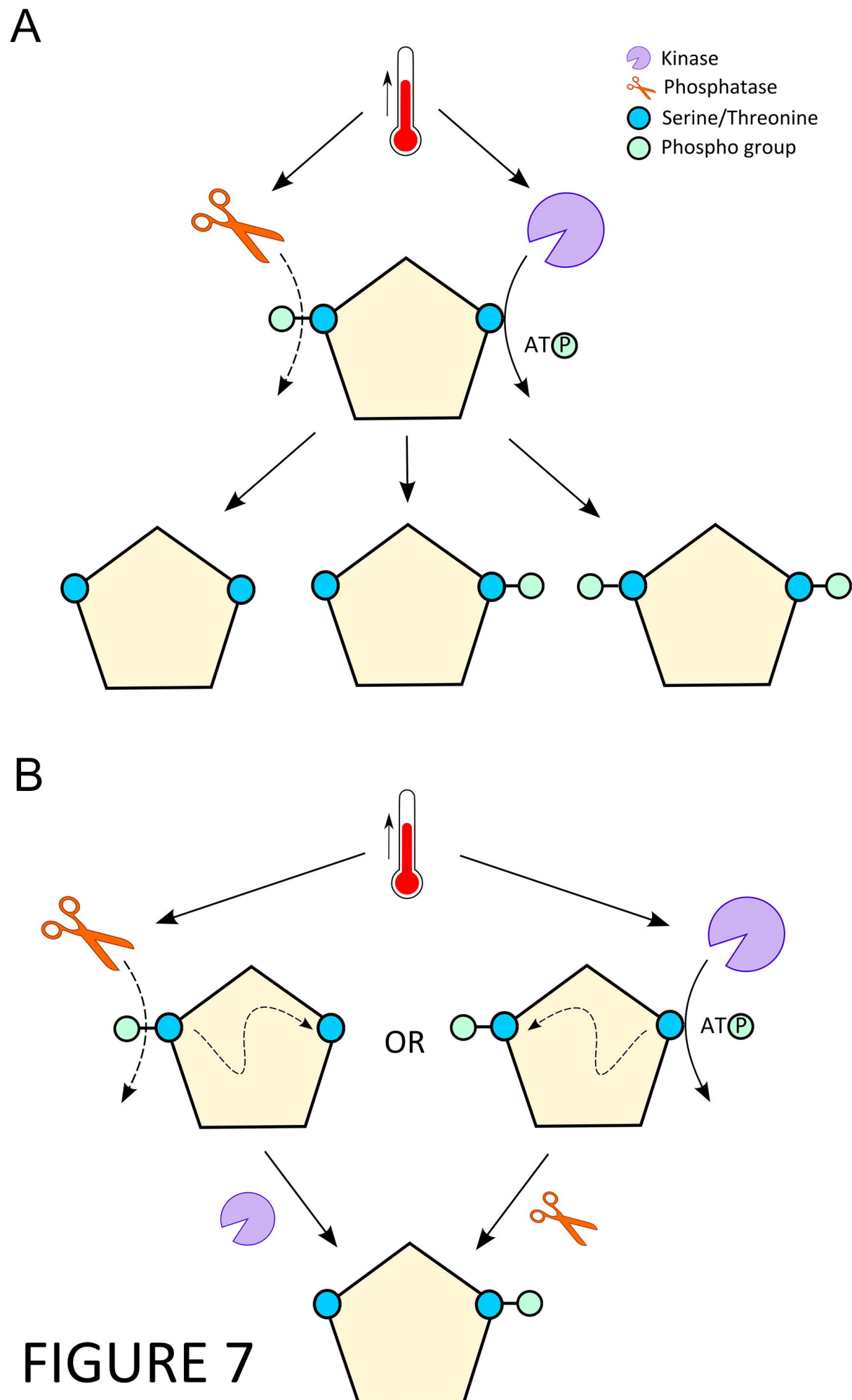
A
Kinase
Phosphatase
Serine/Threonine
Phospho group
ATP
B
OR
ATP

FIGURE 7

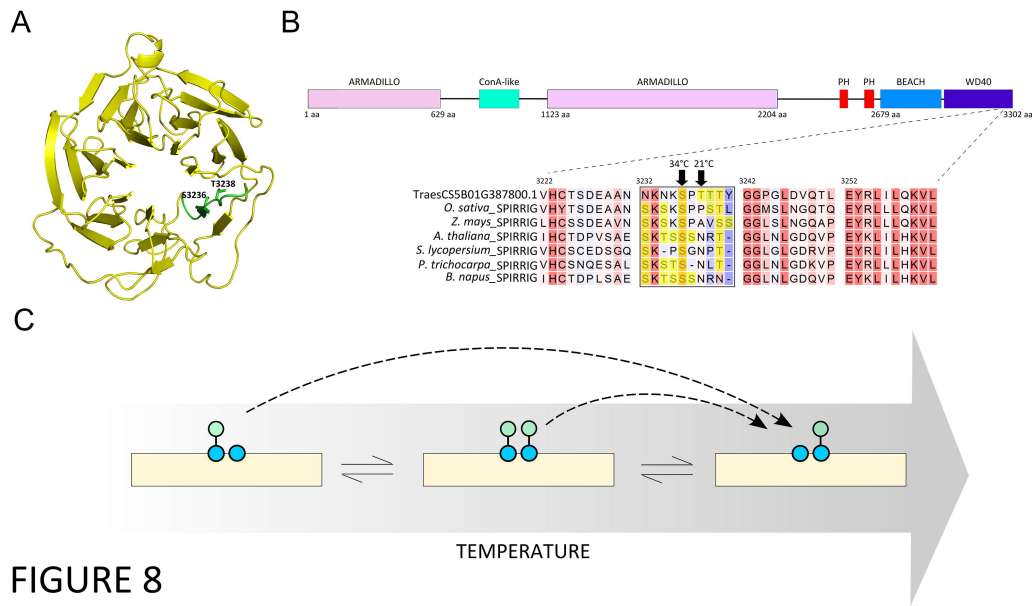
A
T3238
S3236
B
ARMADILLO
ConA-like
ARMADILLO
PH
PH
BEACH
WD40
1 aa
629 aa
1123 aa
2204 aa
2679 aa
3302 aa
34°C
21°C
3222
3232
3242
3252
TraesCS5B01G387800.1 V H C T S D E A A N N K N K S P T T T Y G G P G L D V Q T L E Y R L I L Q K V L
O. sativa_SPIRRIG V H Y T S D E A A N S K S K S P P S T L G G M S L N G Q T Q E Y R L L L Q K V L
Z. mays_SPIRRIG L H C S S D E A V N S K S K S P A V S S G G L S L N G Q A P E Y R L L L Q K V L
A. thaliana_SPIRRIG I H C T D P V S A E S K T S S S N R T E G G L N L G D Q V P E Y K L I L H K V L
S. lycopersium_SPIRRIG V H C S C E D S G Q S K - P S G N P T E G G L G L G D R V P E Y R L I L H K V L
P. trichocarpa_SPIRRIG V H C S N Q E S A L S K S T S - N L T E G G L N L G D K V P E Y R L L L H K V L
B. napus_SPIRRIG I H C T D P L S A E S K T S S S N R N E G G L N L G D Q V P E Y K L I L H K V L
C
TEMPERATURE

FIGURE 8